

APPLICATIONS BULLETIN

New Industrial Calotest for improved coating thickness determination

Introduction

This application note describes the new CSEM Industrial Calotest and its advantages regarding ease of measurement and quality of results. The basic instrument is shown in Fig. 2 together with its electronics unit. The motorised shaft on which the ball rotates is held by an adjustable arm which allows great flexibility in how the ball is positioned on the sample.

For particularly bulky samples which are too big to be mounted in the sample holder provided, the complete arm and motor assembly can be removed and directly clamped to the side of the sample using the magnetic foot provided. The range of rotation speeds of the shaft has been increased to 10 - 3000 rpm for ball diameters between 10 and 30 mm. By keeping the motor assembly away from the electronics has the added advantage of making cleaning much easier than when integrated with the electronics.

Application

The example shown in Fig. 1 is an optical micrograph of a multilayered coating made up of alternate TiN/TiCN deposited on a steel substrate which has been etched in copper sulphate in order to provide sufficient contrast. Testing was carried out with a speed of 1200 rpm for 5 min. and using a steel ball of diameter 30 mm. The ultra-fine diamond paste had an average particle size of 0.1 μm and produced a very high quality scratch-free polish. The coating thicknesses are listed in the figure.

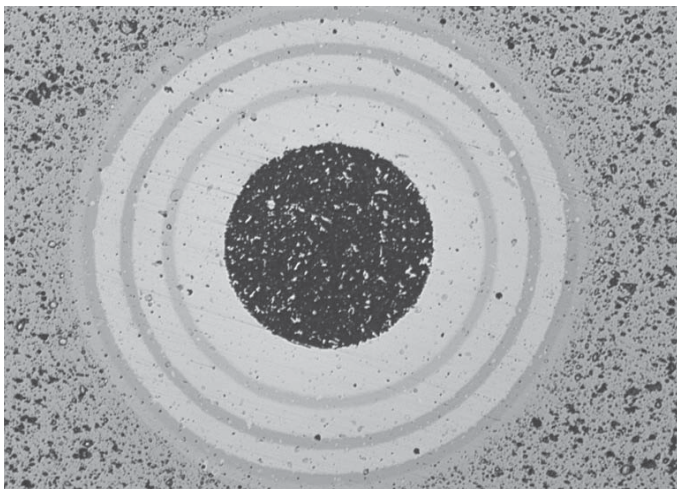


Figure 1 : Optical micrograph of a Calotest performed on a multilayered coating made up of alternate TiN/TiCN deposited on a standard AISI 440C steel substrate. The coating thicknesses are (from the outer ring) 860, 750, 320, 750, 240 and 920 nm.

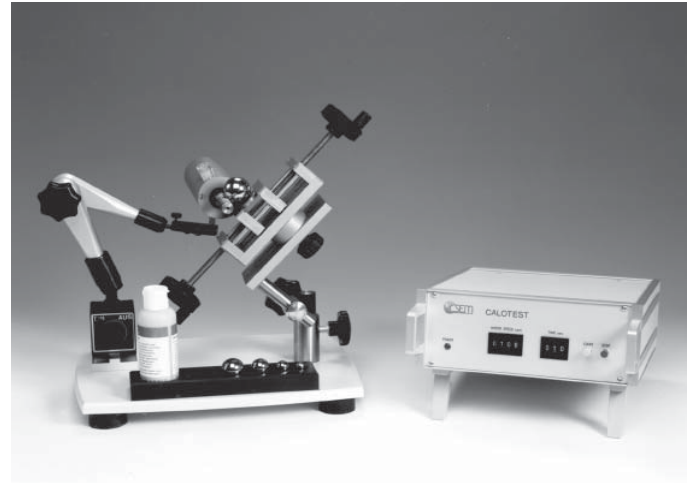


Figure 2 : The Industrial Calotest instrument together with its control unit. Note the adjustable motor arm which enables a large range of sample geometries to be accommodated.

In order to demonstrate the flexibility of the instrument, Fig. 3 shows the result of a Calotest performed on the edge of a milling bit thread. Such a measurement was only possible by using a 10 mm ball for a short time period (30 s). Although an irregular and incomplete wear crater, a coating thickness of 1.93 μm could be accurately determined.

Martin Hess from Eifeler Nord Coating GmbH is acknowledged for providing the optical micrographs in Figs 1 and 3.



Figure 3 : Optical micrographs of a Calotest performed on the thread of a milling bit of diameter 2 mm. Although very small, such a test was possible by using a 10 mm ball with high quality suspension for 30 seconds. Film thickness was found to be 1.93 μm

Micro Hardness Tester (MHT) for fracture toughness determination of brittle materials

Introduction

This application note focusses on the use of a new microindentation instrument, the Micro Hardness Tester (MHT), for determining the fracture toughness of materials by directly measuring Vickers-produced radial cracks as a function of indentation load.

The MHT measuring head (Fig. 2) is designed to exploit the normal force range from 100 mN to 30 N, by using a feedback-controlled force actuator. The resultant displacement of the indenter is measured differentially using a reference fork which remains in contact with the sample during a measurement cycle, giving a total displacement of 200 μm with a resolution of 0.3 nm. A versatile software package allows complete control of the indentation process, including multicycle loading in order to obtain depth-resolved material properties.

Within the context of brittle materials, indentation testing is commonly used for evaluating material toughness, i.e., relating the fracture resistance to the scale of the crack pattern. Although easily applicable to bulk materials, the method is also of importance in understanding the build-up of residual stresses in coated systems as a result of the deposition procedure. The equation relating fracture toughness, K_c , to the post-indentation crack size, c , is given as

$$K_c = \chi \frac{P}{c^{3/2}}$$

where P is the applied indentation load and χ is a constant which depends on the ratio of Young's modulus to hardness, E/H . Most brittle materials generate radial/median cracks which extend from the corners of the residual impression and downwards from the indenter apex.

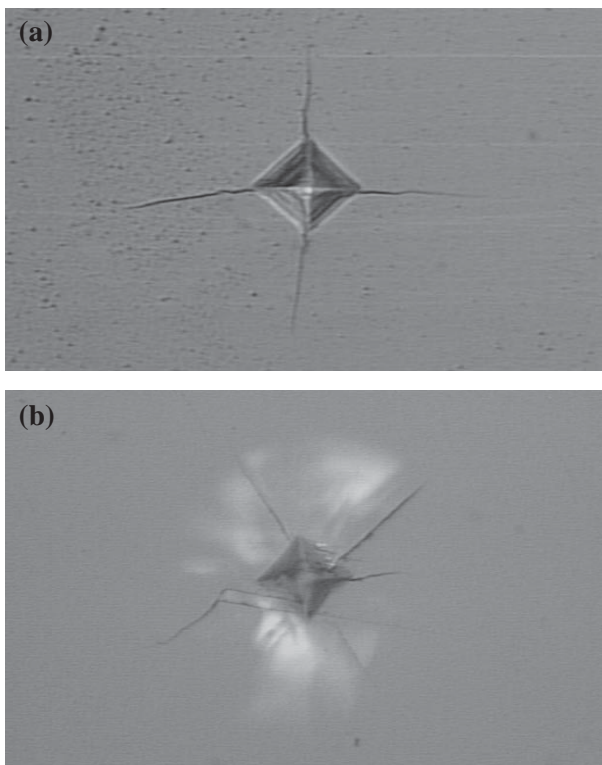


Figure 1 : Optical micrographs of (a) radial cracking in a Si wafer and (b) cracking combined with brittle failure in bulk sapphire (Al_2O_3), for indentations made with applied load 5 N.

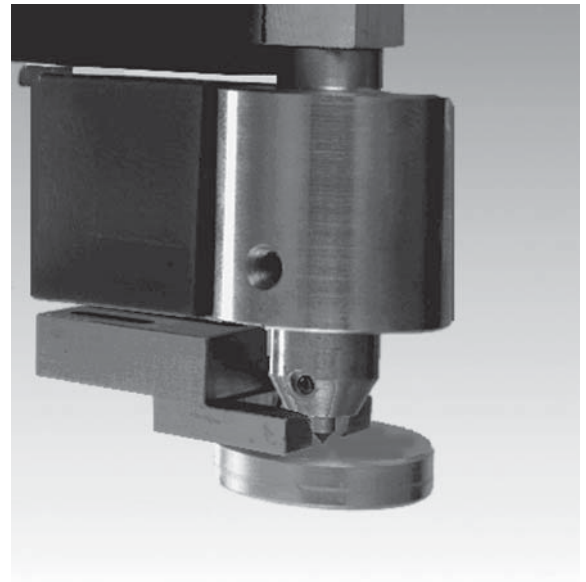


Figure 2 : Principle of the Micro Hardness Tester (MHT) showing the reference fork used for differential measurement of indentation depth.

Application

Fig. 1(a) shows an example of radial cracking in a Si wafer, where the crack lengths can easily be measured using an optical microscope, giving a K_c value of $0.67 \text{ M Pa m}^{1/2}$. However, in the case of indentation into bulk sapphire (Fig. 1(b)), cracking seems to occur randomly around the residual imprint and so an accurate crack length value is difficult to obtain. This phenomenon is due to lateral cracks which spread outward beneath the surface from the deformation zone, causing unwanted interaction with the radial crack system in the form of chipping on the surface. Fig. 3 shows cracking in a TiN coating deposited by CVD onto a steel substrate and it is seen that such cracks are highly reproducible at the corners of the imprint. Quantitative K_c values cannot easily be calculated because of the influence of the substrate on the hardness value, although for comparative studies this is not of great importance.

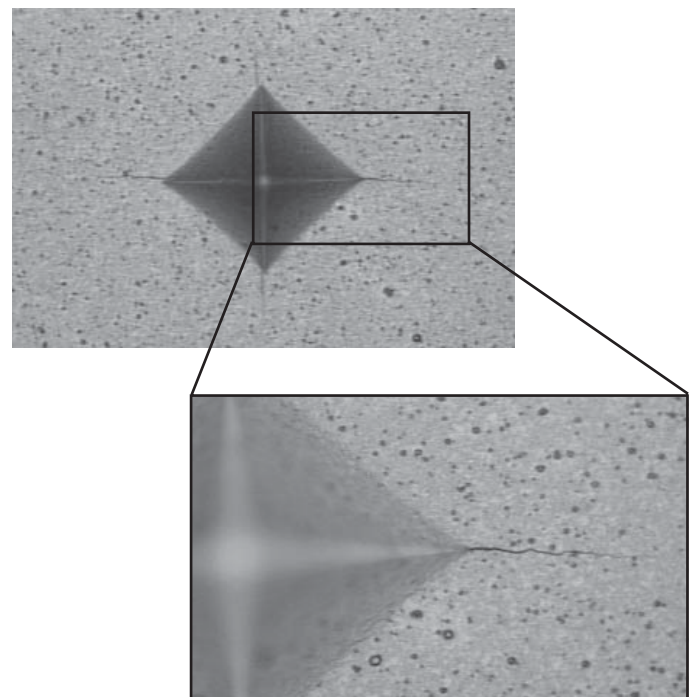


Figure 3 : Optical micrographs of radial cracks emanating from a Vickers indentation (applied load = 20 N) through a TiN coating on a 440C steel substrate. Film thickness is 1 μm .

New Tribometer option for reciprocating wear testing of plasticised tickets

Introduction

This application note features a modification made to a standard CSEM pin-on-disk Tribometer which allows linear reciprocating wear testing to be performed. This option can be particularly useful in applications where linear sliding is a better simulation of true in-service conditions than conventional circular motion.

The main principle of this modified Tribometer is shown in Fig. 2, where a specially adapted block is mounted on frictionless bearings above the circular motor in such a way as to allow movement of the block in a direction perpendicular to the load arm. This set-up gives a theoretical linear speed range of 0.3 - 500 mm s⁻¹, a frequency up to 8.3 Hz and a coupling force of 450 N mm. The maximum applied load which can be used is 46 N.

A good test case for this instrument is the measurement of friction between plasticised tickets as are commonly used in city metro and bus networks. Such tickets are dispensed from automatic machines which are liable to jam if the friction coefficient is too great between two tickets in a stack. In order to optimise the plastified coating which is applied to the tickets, it is important to accurately simulate the dispensing machine with the Tribometer.

In reality, stacks of several hundred tickets are held in a magazine above a feed roller which dispenses them one at a time. By simulating the contact between two tickets, different applied loads can be used in order to find the optimum contact pressure which should be applied by the feed roller to guarantee ticket delivery and eliminate jamming of the dispenser. Obviously, the tribological properties of the tickets will also depend on their processing history as well as environmental changes within the dispenser, e.g., humidity and temperature variations.

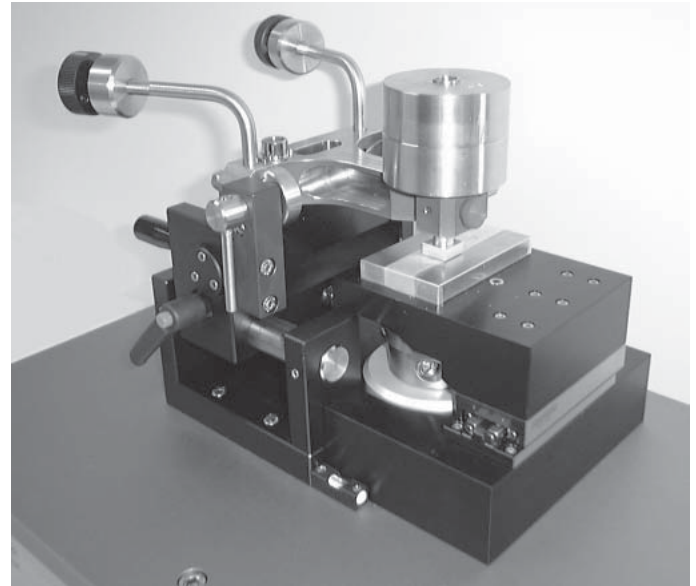


Figure 2 : Principle of the Linear Tribometer showing the standard load arm positioned above the reciprocating sample table.

Experimental

A flat-on-flat conformal contact was chosen in order to best simulate service conditions. For the static partner, a special pin was machined with a square flat at its base (15 x 15 mm) onto which was glued a similar-sized sample cut from the bottom face of a ticket. A complete ticket was then mounted on the sample table with its top side facing the pin. Tests were performed using applied normal loads of 8, 20 and 43 N with sliding speed 10 mm s⁻¹ over a total sliding distance of ~ 60 m. Two different types of ticket were tested and normal laboratory conditions were maintained during all tests (50% RH, 25°C).

Results

The data displayed graphically in Fig. 1 shows an example of a typical raw data set obtained with a normal load of 8 N. As the friction signal is monitored both during the forward and backward movement of the sample, a symmetric trace is obtained of sinusoidal nature. An expanded view of a typical segment is also shown in Fig. 1. After starting with a value of 0.23, the friction coefficient (μ) soon stabilised at a constant value of 0.16 and did not change thereafter even for much longer sliding distances. At loads of 20 and 43 N, the value of μ stabilised at 0.19 and 0.23 respectively.

Interestingly enough, similar tests performed on other ticket batches gave the same results at loads of 20 and 43 N, but could easily be distinguished by their friction coefficient at a load of 8 N. This was therefore the optimum testing condition for this particular mating pair.

Conclusions

The Linear Tribometer has been demonstrated as an ideal testing instrument for particular applications where reciprocating motion is required. It demands little modification to an existing pin-on-disk apparatus and has the advantage of a positive and negative friction measurement from which an average value can be calculated.

Other applications ideally suited to this kind of testing procedure include (i) investigation of friction between a car window and the polymer seal against which it wears over many thousands of cycles; (ii) optimisation of wear in cyclic printing processes; (iii) stick-slip measurements and (iv) wear behaviour in electrical switch contacts.

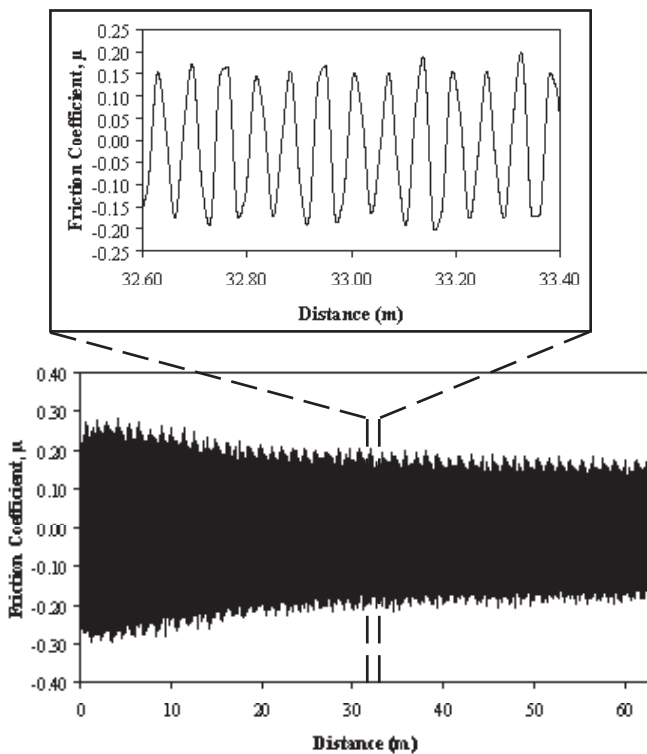


Figure 1 : Raw data from the Linear Tribometer for a test performed between two plasticised tickets with average speed 10 mm s⁻¹ and normal load 8 N over a total sliding distance of 63 m.

Low-load Micro Scratch Tester (MST) for characterisation of thin polymer films

Introduction

In the rapidly expanding field of microelectronics, thin polymeric coatings are often used for both functional and protective reasons where their mechanical properties, and perhaps more specifically their scratch resistance, are of paramount importance. The characterisation of such classes of materials with a scratch testing instrument requires a high resolution in order to monitor the onset of failure, due to the low loads which need to be used.

The modified Micro Scratch Tester (MST), as featured in Application Bulletin No. 3, has proved ideal for low load measurements owing to its upgraded 16 bit acquisition mode. As soft polymeric coatings produce negligible acoustic emission during scratching, the important parameters are usually the tangential force, F_t , and the penetration depth, P_d . The results presented in this application note are for scratch tests performed on various grades of photoresist which are deposited onto Si wafers for lithographic purposes. The coatings had a thickness of $1\ \mu\text{m}$ and differed only in the percentage of additives present in the base PMMA (Polymethyl methacrylate) material. Measurements were made using a Rockwell diamond tip (radius = $100\ \mu\text{m}$), a loading rate of $1\ \text{N min}^{-1}$ over a loading range of 0 - 1 N, giving a scratch length of 10 mm.

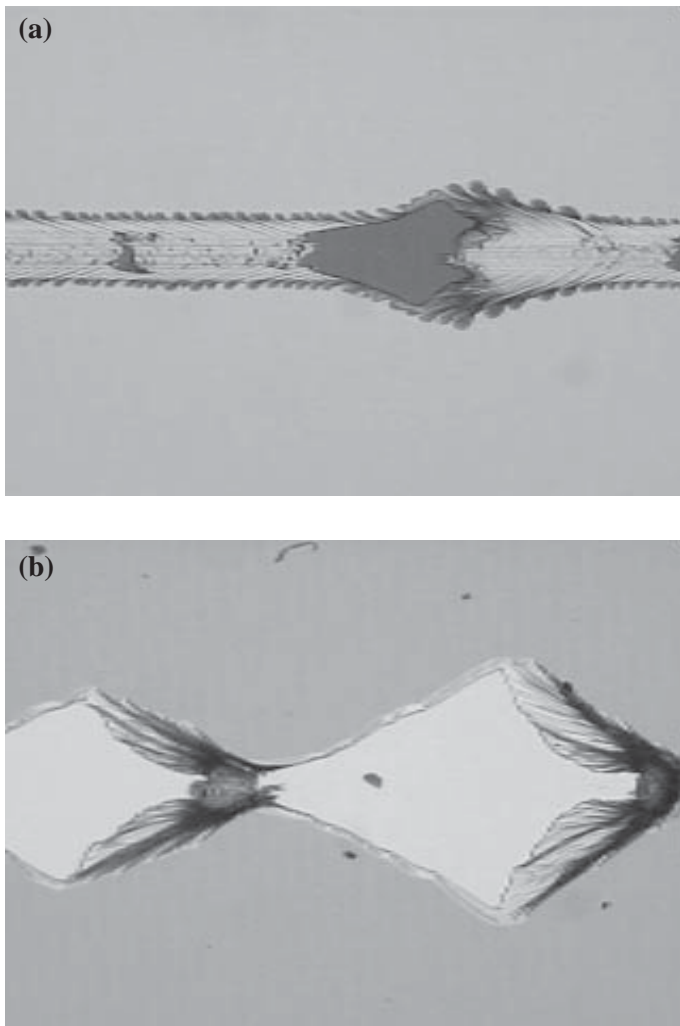


Figure 1 : Optical micrographs of failure modes for two different types of thin polymer film. Both are characteristic of the indenter reaching the substrate and then recovering due to pile-up of material.

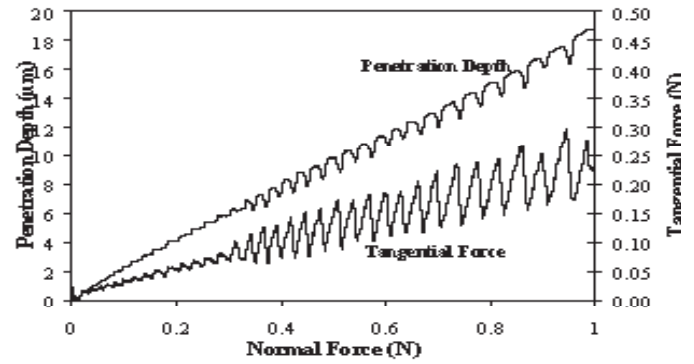


Figure 2 : Typical low-load MST results for a photoresist coating of thickness $1\ \mu\text{m}$ deposited on a Si substrate. The critical failure point of $0.32\ \text{N}$ corresponds to the onset of failure as shown in Fig. 1(b).

Application

The examples in Fig. 1 show the characteristic failure modes encountered when progressive load scratch testing of PMMA coatings. Of particular interest is the manner in which the indenter causes small ruptures on the sides of the scratch path (Fig. 1(a)), after which the substrate is reached. Pile-up of material in front of the advancing indenter then allows the coating to support the applied load for a small distance until the substrate is again reached. For the case of Fig. 1 (b), the critical failure is defined by the first point at which the substrate is reached. Pile-up again causes a small recovery before the substrate is reached for a second time. This cycle continues thereafter with increasing amplitude causing the lozenge-shaped scratch path shown. The corresponding penetration depth and tangential force profiles are shown in Fig. 2. The critical point ($0.32\ \text{N}$) at which the substrate is first reached can clearly be seen on both profiles, as can the increasing amplitude as a function of applied load.



This Applications Bulletin is published quarterly and features interesting studies, new developments and other applications for our full range of mechanical surface testing instruments.

Editor

Dr. Nicholas Randall

Should you require further information, then please contact:

CSM Instruments
Rue de la Gare 4
CH-2034 Peseux
Switzerland

Tel: + 41 32 557 5600
Fax: +41 32 557 5610
info@csm-instruments.com
www.csm-instruments.com

DISTRIBUTOR: